JAERI-M
94-002

INITIAL RESULTS FROM NEUTRON YIELD MEASUREMENTS BY ACTIVATION TECHNIQUE AT JT-60U

January 1994

Magnus HOEK*, Takeo NISHITANI, Yujiro IKEDA
and Atsuhiko MORIOKA

日本原子力研究所
Japan Atomic Energy Research Institute

JAERI-Mレポートは，日本原子力研究所が不定期に公刊している研究報告書です。
入手の問合わせは，日本原子力研究所技術情報部情報資料課（〒319-11茨城県那珂郡東海村）あて，お申しこしください。なお，このほかに財団法人原子力弘済会資料センター（〒319-11 茨城県那珂郡東海村日本原子力研究所内）で複写による実費頒布をおこなっております。

JAERI-M reports are issued irregularly.
Inquiries about availability of the reports should be addressed to Information Division, Department of Technical Information, Japan Atomic Energy Research Institute, Tokai-mura, Naka-gun, Ibaraki-ken 319-11, Japan.

編集兼発行　日本原子力研究所
印　　刷　㈱原子力資料サービス

JAERI-M 94-002

Initial Results from Neutron Yield Measurements by Activation Technique at JT-60U

Magnus HOEK*, Takeo NISHITANI, Yujiro IKEDA
and Atsuhiko MORIOKA

Department of Fusion Plasma Research
Naka Fusion Research Establishment
Japan Atomic Energy Research Institute
Naka-machi, Naka-gun, Ibaraki-ken

(Received January 5, 1994)

The time dependent 2.5 MeV neutron emission from JT-60U plasmas is routinely measured by fission chambers. The neutron yield measurements have now been complemented by time-integrated neutron activation technique utilizing Si-, Al-, In-, Cu-, Zn-, and Ni-foils.

Neutron transport calculations have been performed using Monte Carlo trajectory sampling methods (MCNP code) in order to determine the neutron flux and energy distribution at the irradiation position. In the modeling of the geometry, the importance of the area around the irradiation point has been investigated in detail.

The neutron activation system has just recently been installed at JT-60U. During the high βp experiments, 27-30 July -93, approximately 100 foils were irradiated. The preliminary results of the measurement of the 2.5 MeV neutron yield shows a good agreement with the neutron yield obtained from fission chambers. Among the foils, listed above, indium was the most convenient material due to high sensitivity and relatively low error of the measured neutron yield (∿15%).

The 14 MeV neutron yeild, obtained from fusion between tritium (T) (created from the second branch of fusion between deuterium (DD-reaction)) and deuterium, also gives reasonable values. In this case,

---

* STA Fellowship

silicon and aluminium were the most convenient materials due to high sensitivity, short half lives of the measured daughter nucleus and relatively low errors (∿15-20%).

Keywords: Magnetic Fusion Plasmas, JT-60U, Neutron Yield, Plasma Diagnostics, Neutron Activation Technique, MCNP Code, Neutron Cross Sections, γ-detector Efficiency, γ-detector Sum-coincidence Effects, Triton Burnup

JAERI-M 94-002

JT-60Uにおける放射化箔法中性子発生量測定の初期結果

日本原子力研究所那珂研究所炉心プラズマ研究部
Magnus HOEK*・西谷　健夫・池田裕二郎・森岡　篤彦

（1994年 1 月 5 日受理）

JT-60Uではプラズマから発生する2.5 MeV 中性子の時間変化を定常的に核分裂電離箱で測定している。ここでは，1放電当りの積算中性子発生量をシリコン，アルミニウム，銅，亜鉛，ニッケルの箔を用いた中性子放射化法により測定した。

軌跡サンプリングモンテカルロ法（MCNP コード）を使用した中性子輸送計算により，照射位置での中性子フルエンスと中性子エネルギー分布を決定した。モデル化においては照射位置周辺領域の重要性を詳細に調べた。

JT-60Uでは中性子放射化箔システムを最近導入した。これにより1993年7月27～30日の高ポロイダルベータ実験時に，約100の箔を照射した。2.5 MeV 中性子発生量の初期測定結果は核分裂電離箱で測定した中性子発生量と良く一致することを確認した。上に示した箔のうち，インジウム箔は高感度であるため全中性子発生量測定に最も適しており，測定誤差は～15%である。

重水素・重水素反応の2次生成物であるトリチウム（T）と重水素との核融合反応で生じる14 MeV中性子発生量もまた妥当な値を得ている。この測定には，シリコンとアルミニウムが高感度かつ測定する娘核種の半減期が短いため最も適しており，測定誤差は～15 -20 %である。

那珂研究所：〒311－01　茨城県那珂郡那珂町向山801－1
＊　原子力交流制度研究員

Contents

目　　次

1. Introduction

The total neutron yield is a suitable parameter for the evaluation of the plasma performance. In normal cases of DD burning plasma operation, the neutrons are mainly generated from fusion between two deuterium ions. Therefore, the 2.5 MeV neutron represents an occurred fusion reaction. The total time-resolved neutron yield is routinely measured by calibrated fission chambers at JT-60U [1]. Another way of measuring neutron yields is neutron activation of different materials with well known neutron interaction cross-sections. Furthermore, by using threshold reactions, it is possible to distinguish between DD-neutrons (2.5 MeV) and DT-neutrons (14 MeV). The 14 MeV neutrons are created when the tritons, which comes from the second branch of the DD-reaction, slow down and undergo a DT fusion reaction.

The sample to be irradiated, is positioned very close to the plasma (~2.5 m) using a pneumatic rabbit system. After removal of the sample, the induced radioactivity is measured using a high-resolution semiconductor diode (HP-Ge crystal). If the efficiency of the γ-detector is known then, from the area under the measured γ-peak, the neutron flux at the sample can be derived. In order to calculate the total neutron yield from the plasma, the relation between the neutron flux at the irradiation position and total neutron yield from the whole plasma region, has to be known. This has been achieved by using Monte Carlo trajectory sampling methods, the MCNP code [2].

Table 1. *Neutron induced reactions used for the neutron activation at JT-60U. The columns show the isotopic abundance for the isotope of interest and the half-life in minutes [m], hours [h], or days [d] for the radioactive daughter nuclide. Also shown is the energy of the γ-line with its γ-abundance. Finally, the threshold neutron energy and the energy at the maximal cross-section is given.*

Reaction	Isotopic Abund. [%]	Half-life	Gamma Energy [MeV]	Gamma Abund. [%]	Thresh. Energy [MeV]	Energy at max X-section [MeV]
115In(n,n')115In	95.7	4.49 h	0.336	45.9	0.3	2.8
64Zn(n,p)64Cu	48.6	12.70 h	0.511	37.8	1	11.2
58Ni(n,p)58Co	68.3	70.8 d	0.811	99.4	0.00005	8.6
27Al(n,p)27Mg	100.0	9.46 m	0.844	73.0	1.8	10.1
63Cu(n,2n)62Cu	69.2	9.73 m	0.511	195.0	11.1	> 16
28Si(n,p)28Al	92.2	2.24 m	1.779	100.0	4	10.4
27Al(n,alpha)24Na	100.0	15.02 h	1.369	100.0	3.1	13.1
58Ni(n,2n)57Ni	68.3	36.0 h	1.378	77.6	12.2	16.1

Table 1 shows the neutron induced reactions which have been used so far. From the neutron threshold energy and from the neutron energy at which the cross-section is maximum, it is evident that the $^{115}In(n,n')^{115m}In$ -, $^{64}Zn(n,p)^{64}Cu$ - and $^{58}Ni(n,p)^{58}Co$-reactions are suitable for measurements of the 2.5 MeV neutron yield. The $^{27}Al(n,p)^{27}Mg$ reaction has a threshold very close to 2.5 MeV while the maximum cross section occurs at 10 MeV. In the case of indium, the activity produced by the $^{115}In(n,n')^{115m}In$ reaction are determined by counting the 336 keV γ-line of the ^{115m}In decay. The maximum of the activation cross section occurs around 2.8 MeV so that the influence of scattered neutrons of degraded energies is reduced. As stated before, the 2.5 MeV neutron yield measurements are conveniently measured by the fission chambers. However, the yield measured by foil activation is to be used as cross calibration for the fission chambers.

When deuterium ions fuse, the reactions $D(D,n)^3He$ and D(D,p)T have equal probability. This means that tritons (T) are generated in the same rate as 2.5 MeV neutrons. The generated 1 MeV triton in the second reaction is of interest due to its similar kinematics to the 3.5 MeV α-particles which will be used for the heating of the plasma in a future commercial fusion reactor. When the confined tritons are slowing down and thermalized in the plasma, a T(D,n)α reaction is possible ("triton burnup"), thereby generating a 14 MeV neutron which can be measured. The flux of these 14 MeV neutrons depends on the slowing down of the tritons and how well the tritons are confined. The confinement of the tritons should depend on the plasma current and different particle loss mechanisms. The fractional losses of 1 MeV tritons have been calculated using a Orbit Following Monte Carlo code (OFMC). In JT-60U the loss of tritons is expected to be higher than in JET and in TFTR due to its large toroidal field ripple (ripple losses) and due to the orientation of the neutral beam injection (NBI) which is nearly perpendicular to the toroidal magnetic field. The fractional loss of tritons in JT-60U have been calculated to ~45% for a plasma current of 1.5 MA [3]. The final amount of tritons which are slowed down, confined and reacting with deuterium is ~1%. Therefore, the fraction of 14 MeV neutrons to 2.5 MeV neutrons is expected to be in the range of 1%.

The slowing down time of the tritons and the yield of the 14 MeV neutrons may be measured using a silicon surface barrier detector (SBD) [3,4]. However, due to the intense 2.5 MeV neutron flux, this kind of detector soon has to be replaced due to radiation degradation. Another way, for the measurement of the yield, is by utilizing foil activation.

From table 1 it is realized that the reactions $^{63}Cu(n,2n)^{62}Cu$, $^{28}Si(n,p)^{28}Al$, $^{27}Al(n,\alpha)^{24}Na$ and $^{58}Ni(n,2n)^{57}Ni$ have threshold reactions higher than 2.5 MeV and are therefore suitable for the measurements of the 14 MeV neutrons. Silicon should be very suitable for monitoring this weak emission. The daughter nuclide, ^{28}Al, has a half-life of 2.24 min. and is therefore suitable for studying discharges of up to 1 minute duration. The decay γ-radiation has an energy of 1.779 MeV and is easily measured by a HP-Ge detector. Due to the short half-life, the same sample can also be recycled after a cooling time of only ~30 min.

2. Basic Theory

Most species in nature becomes radioactive during neutron irradiation. The activity can be measured by detecting the emitted particles such as β-particles or photons.

If we assume an unperturbed neutron flux (thin sample), the reaction rate, R, is given by:

$$R = \Phi \Sigma_{act} V \quad [s^{-1}] \qquad [1]$$

where Φ $[s^{-1} \cdot cm^{-2}]$ is the neutron flux averaged over the sample surface,
Σ_{act} $[cm^{-1}]$ is the activation cross section averaged over the neutron spectrum and
V $[cm^3]$ is the volume of the sample.

If we assume that R is constant and that "burn-up" of target nuclei is negligible, then the number of radioactive nuclei, N, can be written as:

$$N(t) = \frac{R}{\lambda}(1 - e^{-\lambda t}) \quad N = 0 \text{ at } t = 0 \qquad [2]$$

where λ is the decay constant of the created daughter nuclide.

The activity (disintegration rate), A, of the sample after irradiation time, t_0, is given by:

$$A(t_0) = \lambda N(t_0) = R(1 - e^{-\lambda t_0}) \equiv A_0 \quad [s^{-1}] \qquad [3]$$

After irradiation, the sample is transferred to a γ-detector and the counts, C, under the specific γ-line is measured. If the measurement time is $\Delta t = t_2 - t_1$ then the number of measured γ-counts can be written as:

$$C = \alpha_\gamma \varepsilon \int_{t_1}^{t_2} A_0 e^{-\lambda t} dt = \alpha_\gamma \varepsilon A_0 \frac{e^{-\lambda t_1}}{\lambda}(1 - e^{-\lambda \Delta t}) \qquad [4]$$

where α_γ is the γ-abundance and
ε is the efficiency of the γ-detector.

From eqs. [3] and [4], the reaction rate, R, can now be calculated by:

$$R = \frac{A_0}{1 - e^{-\lambda t_0}} = \frac{\lambda \cdot C}{\alpha_\gamma \cdot \varepsilon \cdot e^{-\lambda t_1}(1 - e^{-\lambda \Delta t})(1 - e^{-\lambda t_0})} \quad [s^{-1}] \qquad [5]$$

Equation [5] can be simplified by assuming that $t_0 << 1/\lambda \propto t_{1/2}$ *i.e.* the irradiation time is much shorter than the half-life of the radioactive nucleus (typical irradiation times are 1-5 s.). Furthermore, if eq. [5] is multiplied with the irradiation time, t_0, then we get an expression for the total number of reactions from the irradiation:

$$N = R \cdot t_0 \approx \frac{C}{\alpha_\gamma \cdot \varepsilon \cdot e^{-\lambda t_1}(1 - e^{-\lambda \Delta t})} \qquad [6]$$

Figure 1 shows the activity of a sample during and after irradiation. Note that t_1 is the time after the irradiation has stopped, *i.e.* the "cooling time" of the sample.

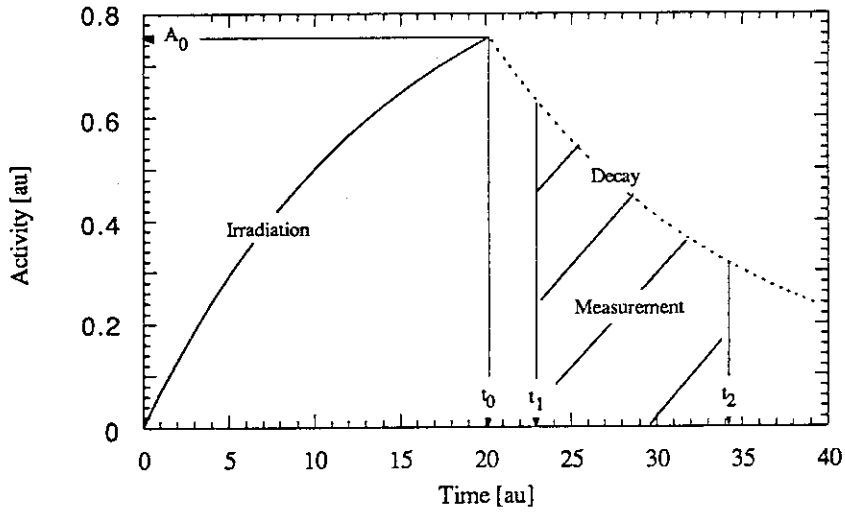

Fig.1. *Irradiation and following decay for a neutron activated sample. The activity after irradiation is A_0 at time t_0. After a certain cooling time, t_1 (in the figure the cooling time is actually t_1-t_0), the γ-measurement starts and continues until t_2.*

For the measurement of the total neutron yield from the plasma, we have to calculate the relation between the neutron flux at the irradiation position and the total emitted neutron flux. The reaction rate with the sample can be written as (*cf.* eq. [1]):

$$R = nV \int_0^{E_0} \Phi(E)\sigma(E)dE \quad [s^{-1}] \qquad [7]$$

where n is the number of interesting nuclei per unit volume of the sample,
V is the volume of the sample,
$\Phi(E)$ is the flux at the irradiation point,
$\sigma(E)$ is the cross section for the neutron reaction and
E is the neutron energy.

If $\Phi^*(E)$ is the neutron flux/source neutron at the irradiation position, we have:

$$\Phi(E) = S_n \Phi^*(E) \qquad [8]$$

where S_n is the total number of emitted source neutrons.

From eqs. [7] and [8] we then get an expression for the total time integrated neutron yield:

$$S_n = \frac{R}{nV \int_0^{E_0} \Phi^*(E)\sigma(E)dE} \cdot t_0 = \frac{N}{nV \int_0^{E_0} \Phi^*(E)\sigma(E)dE} \qquad [9]$$

Here, N is given by eq. [6] while the integral ("flux integral") is approximately given by:

$$\int \Phi^*(E)\sigma(E)dE \approx \sum_i \Phi^*(E_i) \cdot \sigma(E_i) \qquad [10]$$

The number of nuclei per unit volume, n, can be expressed as

$$n = \alpha_{IS} \cdot \frac{m}{V} \cdot \frac{N_A}{M} \qquad [11]$$

where α_{IS} is the isotopic fraction of the nuclide,
m is the mass of the sample,
N_A is Avogadro's constant (6.023×10^{23}) mole^{-1} and
M is the molar mass of the nuclide.

Equations [6], [9], [10] and [11] then give us the final equation for the calculation of the time integrated neutron yield:

$$S_n = \frac{C \cdot M}{\alpha_\gamma \cdot \varepsilon \cdot e^{-\lambda t_1} \cdot (1 - e^{-\lambda \Delta t}) \cdot \alpha_{IS} \cdot m \cdot N_A \sum_i \Phi^*(E_i)\sigma(E_i)} \qquad [12]$$

The energy distribution of the neutron flux/source neutron, $\Phi^*(E_i)$, has been calculated by MCNP, assuming mono-energetic source neutrons. Figures 2 and 3 show the flux per source neutron and MeV as a function of neutron energy for 2.45 MeV and 14.1 MeV source neutron energies. Also shown, are the tabulated cross sections [barn]. The used cross sections have been measured by FNS [5] and will be included in JENDL Activation File in Jan. -94.

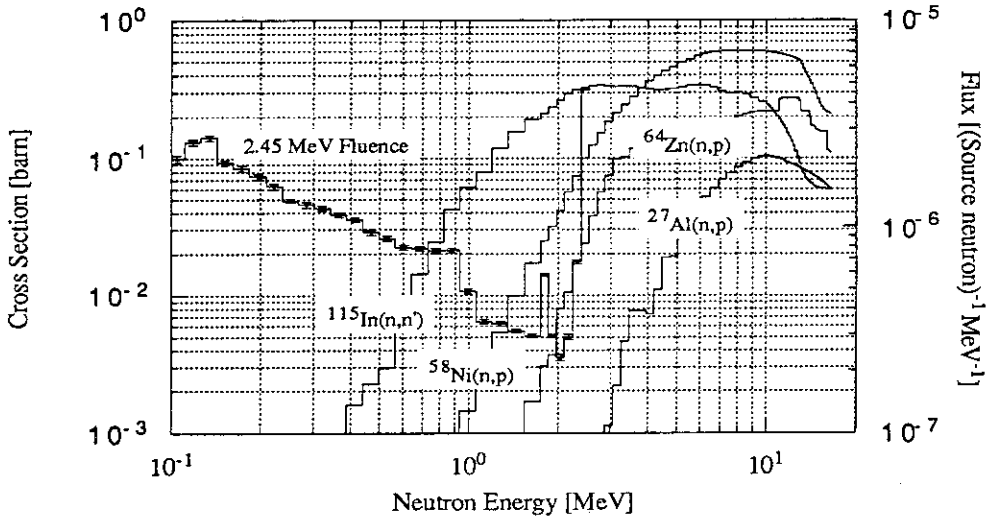

Fig.2. Neutron cross-sections for the "2.5 MeV" foils and the neutron flux from the JT-60U Tokamak. The neutron flux is obtained from MCNP calculations, assuming mono-energetic 2.45 MeV source neutrons. The error bars of the neutron flux are the statistical errors from the Monte Carlo calculations.

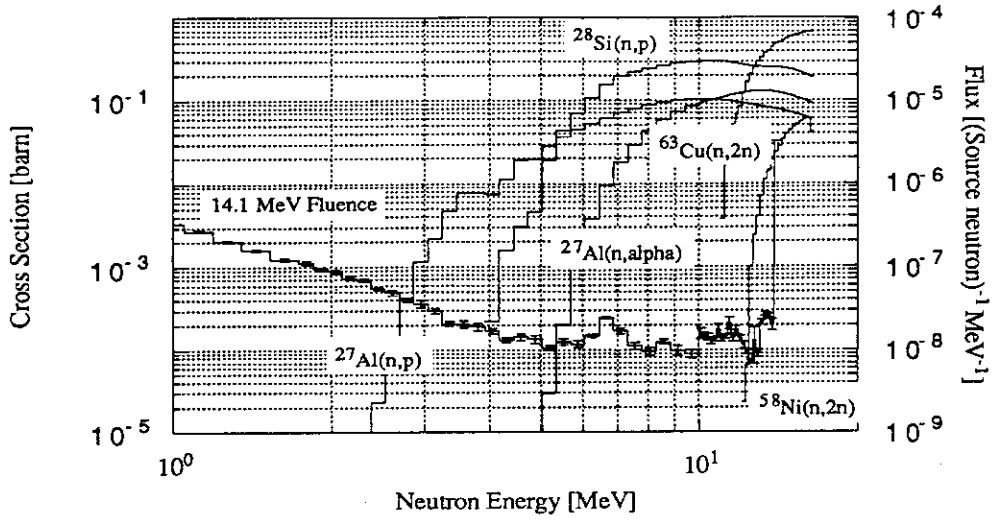

Fig.3. Neutron cross-sections for the "14 MeV" foils and the neutron flux from the JT-60U Tokamak. The neutron flux is obtained from MCNP calculations, assuming mono-energetic 14.1 MeV source neutrons. The error bars of the neutron flux are the statistical errors from the Monte Carlo calculations.

When the 2.5 MeV neutron yield is measured using indium-, zinc-, nickel-, or aluminium- foils, the weak emission from non scattered and scattered 14 MeV source neutrons also contribute to the measured yield. This contribution can be roughly estimated using the relation between the flux integrals. Furthermore, if we assume that the "triton burnup" is 1%, we get the contribution from non scattered and scattered 14 MeV neutrons by (*cf.* eq. [12]):

$$\frac{S_n(14.1)}{S_n(2.45)} = \frac{C_\gamma(14.1)}{C\gamma(2.45)} \cdot \frac{\int_{0.1}^{2.45} \Phi^*_{2.45}(E)\sigma(E)dE}{\int_{0.1}^{14.1} \Phi^*_{14.1}(E)\sigma(E)dE} \equiv 1\% \qquad [13]$$

where C_γ is the measured γ-counts from neutron reactions with non scattered and scattered 2.5 and 14 MeV source neutrons The lower energy limit, 0.1 MeV, is the cutoff neutron energy in the MCNP calculations.

Table 2 shows the calculated flux integrals for the reactions of interest. From table 2 it is evident that the contribution to the measured γ-counts, from the 14 MeV neutron yield, is negligible for all foils except the aluminium foil and maybe the zinc foil. This fact makes it difficult to use the ^{27}Al(n,p) reaction for the measurement of the 2.5 MeV neutron yield if the "triton burnup" is not known. In fact the ^{27}Al(n,p) reaction is more suitable for measurements of the 14 MeV neutron yields. On the other hand, if the "triton burnup" has been measured by irradiation of *e.g.* silicon or copper foils, the 2.5 MeV yield from the ^{27}Al(n,p) reaction could be used as a cross check of the triton burnup. The measured counts, C, shall then be corrected according to:

$$C_{2.45} = \frac{C}{1+"Burnup" \cdot \frac{\int_{0.1}^{14.1} \Phi^*_{14.1}(E)\sigma(E)dE}{\int_{0.1}^{2.45} \Phi^*_{2.45}(E)\sigma(E)dE}} \qquad [14]$$

where the value of $C_{2.45}$ shall be used in eq. [12] for the measurement of the 2.5 MeV neutron yield.

Table 2. *Calculated flux integrals, eq. [10], for the "2.5 MeV foils". Also shown, is the contribution [%] from scattered and non scattered 14 MeV source neutrons to the measured number of γ-counts, assuming a triton burnup of 1%.*

Reaction	Flux Integral 0.1-2.45 MeV [1E-24]	Flux Integral 0.1-14.1 MeV [1E-24]	Fraction of "14 MeV g-counts" at 1% triton burnup [%]
115In(n,n')115mIn	3.42E-07	1.34E-07	0.4
64Zn(n,p)64Cu	1.96E-08	1.72E-07	8.8
58Ni(n,p)58Co	8.59E-08	3.45E-07	4.0
27Al(n,p)27Mg	1.67E-11	6.51E-08	3898.2

Finally, it is of interest to know how the sensitivity of the samples are related to each other. If we assume that we want to measure the irradiated sample for 20 minutes, then we can calculate the necessary total emitted neutron yields using eq. [12]. The results from these calculations are shown in figs. 4 and 5.

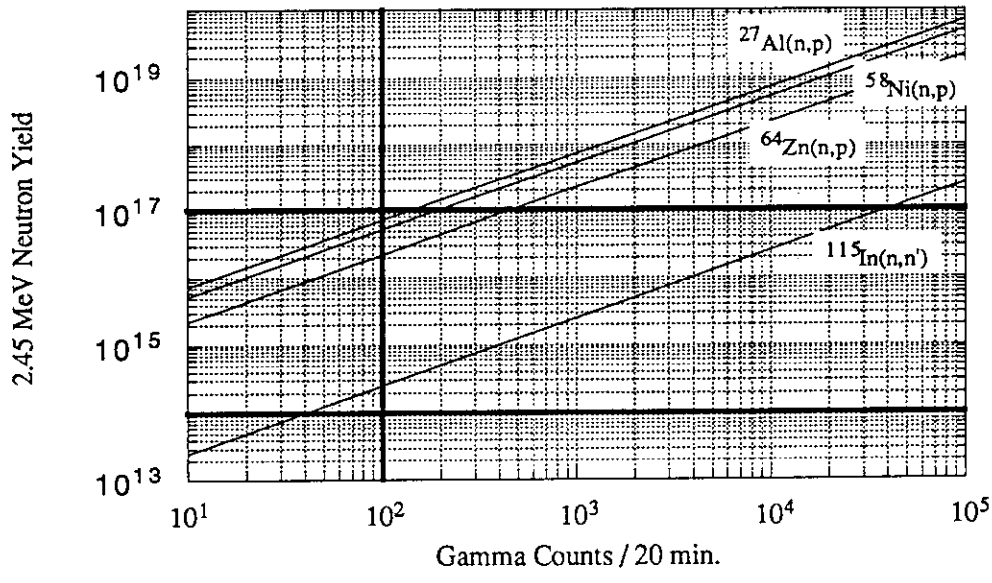

Fig.4. *Calculated necessary neutron yields (cf. eq. [12]) from the JT-60U Tokamak as a function of measured γ-counts for the "2.5" MeV foils. The assumed data for the calculated yields are shown in table 3.*

The normal total neutron yield from the JT-60U Tokamak during deuterium beams on deuterium plasma is also indicated (10^{14} - 10^{17} neutrons) in figs. 4 and 5. If we assume 1% triton burnup, this should correspond to 10^{12} - 10^{15} 14 MeV neutrons. Also indicated, is the wanted minimum number of γ-counts for a measurement time of 20 min. (100 counts minimum). The necessary data for the calculations are shown in table 3.

From fig. 4 it is evident that indium is the most sensitive foil for the 2.5 MeV neutrons. The minimum total neutron yield is ~5×10^{14} neutrons. However, the zinc foil should also give sufficient statistics of the γ-counts for higher neutron yields. Utilizing nickel and aluminium foils, demands very high neutron yields (> 10^{17} neutrons).

Figure 5 indicates that the copper foil should be most suitable for the measurement of the 14 MeV neutron yield. However, copper foils demands two successive γ-measurements (see section "Results") and therefore the silicon and aluminium foils are more suitable due to its measurement simplicity. The nickel foil, again, demands very high neutron yields to give any useful γ-counts.

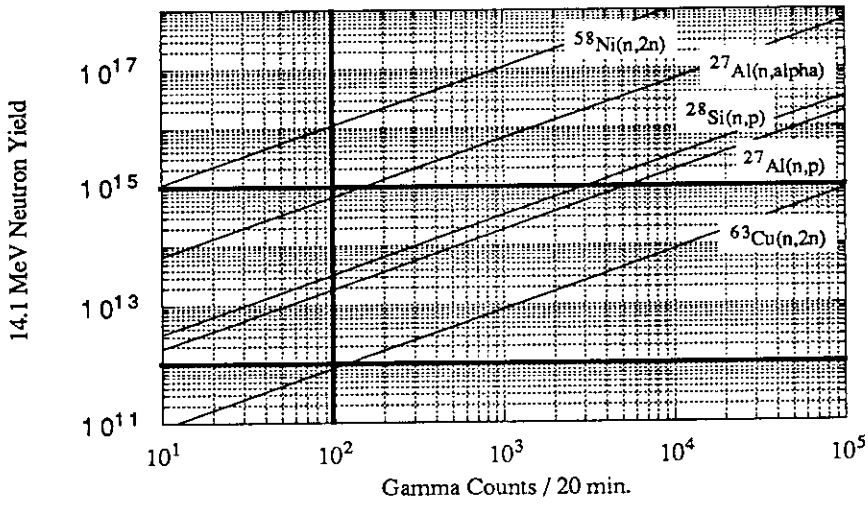

Fig.5. *Calculated necessary neutron yields (cf. eq. [12]) from the JT-60U Tokamak, as a function of measured γ-counts for the "14" MeV foils. The assumed data for the calculated yields are shown in table 3.*

Table 3. *Assumed data for the results shown in figs. 4 and 5. The masses of the samples are typical for the neutron yield measurements done so far. The third column shows the energy of the source neutrons used for the calculations of the flux integral, see eq. [10]. The cooling time of the samples and the assumed measurement times are shown in columns 4 and 5. The efficiency of the HP-Ge detector are based on the assumptions described in section "Efficiency of the γ-detector".*

Reaction	Mass [g]	Energy [MeV]	Cooling [h]	Meas. Time [min.]	Efficiency [%]	Flux Integra [1E-24]
115In(n,n')	0.3	2.45	5	20	7.20	3.42E-07
64Zn(n,p)	0.2	2.45	5	20	4.94	1.96E-08
58Ni(n,p)	0.7	2.45	60	20	3.42	8.59E-08
27Al(n,p)	0.2	2.45	0	20	3.32	1.67E-11
63Cu(n,2n)	0.7	14.1	0	20	4.94	3.48E-07
27Al(n,p)	0.2	14.1	0	20	3.32	6.51E-08
28Si(n,p)	0.04	14.1	0	20	1.87	2.05E-07
27Al(n,alpha)	0.2	14.1	0	20	2.26	9.68E-08
58Ni(n,2n)	0.7	14.1	0	20	2.25	1.69E-08

3. Efficiency of the γ-detector

For the efficiency calibration of the HP-Ge detector, a set of calibration sources have been used, see table 4. If the detector efficiency is ε and the branching ratio of the γ-line is α_γ, then the measured counts, from time t_1 to t_2, can be written as:

$$C = \alpha_\gamma \varepsilon A_0 \int_{t_1}^{t_2} e^{-\lambda t} dt = \alpha_\gamma \varepsilon A_0 \frac{e^{-\lambda t_1}}{\lambda}(1 - e^{-\lambda \Delta t}) \qquad [15]$$

where A_0 [Bq] is given by the manufacturer of the calibration sources [6],
t_1 is the cooling time of the γ-source and
Δt is the measurement time.

If the measurement time $\Delta t = t_2 - t_1$ is short compared to the half-life of the source, the measured efficiency can be written as:

$$\varepsilon \approx \frac{C}{\alpha_\gamma A_0 e^{-\lambda t_1} \Delta t} \qquad [16]$$

Table 4 *Calibration sources used for the efficiency calibration of the HP-Ge detector. The half-lives are given in days [d] and years [y].*

Source	Gamma (keV)	Abundance (%)	Half-life	Activity A0 30-Jun-93 (kBq)
Am-241	59.54	35.90	432.7 y	44.80
Co-57	122.06	85.68	271.77 d	42.08
Co-57	136.47	10.67	271.77 d	42.08
Cr-51	320.08	9.85	27.703 d	21.75
Na-22	511.00	90.57	2.602 y	37.22
Sr-85	514.01	99.29	64.85 d	36.74
Cs-137	661.66	84.70	30.15 y	42.72
Mn-54	834.84	99.98	312.2 d	52.43
Y-88	898.04	93.70	106.62 d	42.77
Co-60	1173.24	99.89	5.271 y	36.04
Na-22	1274.54	99.93	2.602 y	37.22
Co-60	1332.50	99.98	5.271 y	36.04
Y-88	1836.06	99.37	106.62 d	42.77

However, the measured efficiencies determined with a HP-Ge detector, can be incorrect unless the source-detector distance is several times the detector radius. This effect is a consequence of either summation of coincidental γ-rays or complete or partial energy loss in the detector. As an example of summation effect, fig. 6 shows the decay scheme of ^{60}Co.

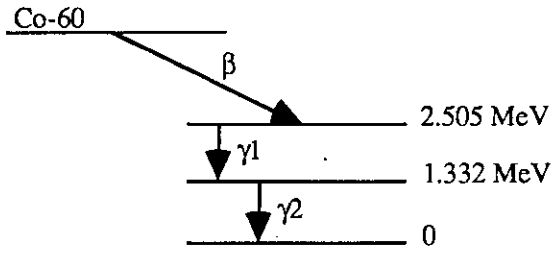

γ1: 1.173 MeV 100%
γ2: 1.332 MeV 100%

***Fig.6**. Decay scheme of ^{60}Co. Two photons are emitted in coincidence, with energies 1173 keV and 1332 keV. Apart from the two measured peaks at these energies, a summation peak may also appear at 2505 keV.*

The γ_1- and γ_2- lines in fig. 6, are used for the efficiency measurements. If, however, both the coincidental γ_1 and γ_2 are registered by the detector, the true count from either γ_1 or γ_2 are lost, giving a too low measured efficiency. Table 5 shows the contribution from summation for some measured γ-sources. In the case of ^{137}Cs it is interesting to note that we also have summation between non-coincidental γ-lines (662 keV). This is probably due to the long half-life (2.5 min.) of the excited state of the daughter nucleus. Anyway, it is clear that the loss of γ-counts due to summation is evident. However, when comparing the count-rates from the "true" γ-peaks with the summation peaks, it seems as summation is not important. However, it should be emphasized that the count-rates, given in table 5, only describe those situations where the complete summed γ-energy is detected. The amount which is partially detected, ends up in the background together with the Compton energy distribution and is unknown.

Figure 7 shows the measured efficiency (dotted lines) as a function of channel (~0.5 keV/channel) for the calibration sources. The 511 keV γ-line from ^{22}Na has been omitted due to the unavoidable present background of 511 keV γ-rays and the difficulty in measuring annihilation radiation. It is clear, that for short distances between calibration source and detector (surface, 1st and 2nd pos.), the efficiency drops due to summation effects. It seems, as this is especially apparent for ^{88}Y.

Table 5 *Table with the measured count-rates for some of the used calibration sources. The type of source with it's γ-energies and γ-abundance's are shown in the first three columns. Columns 4 and 5 contain the count-rates for the closest position (1^{st}) and the furthest position (4^{th}) relative to the γ-detector. The last three columns contain the measured summation peaks with it's count-rates. A "?" indicates that the value is not measurable, due to the fixed amplification (~0.5 keV/channel, 4096 channels).*

Source	g-peaks [keV]	g-abund. [%]	Rate [cps] 1st pos.	Rate [cps] 4th pos.	Sum peaks [keV]	Rate [cps] 1st pos	Rate [cps] 4th pos.
Co-57	122	85.68	4210.16	259.23	258	6.36	0.00
	136	10.67	515.34	32.31			
Cs-137	662	84.70	1321.39	93.68	1322	1.42	0.00
Y-88	898	93.70	863.60	68.75	2734 ?	?	?
	1836	99.37	492.93	41.22			
Co-60	1173	99.89	662.37	57.88	2505 ?	?	?
	1332	99.98	594.27	52.28			
Na-22	511	90.57	1808.98	187.57	1785	49.78	0.30
	1275	99.93	524.92	55.02			

Most irradiated foils are measured at the 1st position. Therefore, it is necessary to correct for the summation effects. We see from fig. 7 that the summation effects decrease with an increased source-detector distance. This can also be realized analytically.

In the case of two γ-lines in coincidence and assuming absence of summation between the two γ-lines, the full-energy peak counts, N, can be written as:

$$N_1 = \varepsilon_1 \Omega S \alpha_{\gamma_1} \qquad [17]$$

$$N_2 = \varepsilon_2 \Omega S \alpha_{\gamma_2} \qquad [18]$$

where ε is the efficiency of the detector,
Ω is the solid angle subtended by the detector surface,
S is the number of disintegration's and
α_γ is the yield of the γ-ray per disintegration.

The number of summation counts can then be written as:

$$N_{12} = S \cdot \varepsilon_1 \varepsilon_2 \cdot \alpha_{\gamma_1} \alpha_{\gamma_2} \cdot \Omega^2 \propto \Omega^2 \qquad [19]$$

Due to that the number of summation counts is $\propto \Omega^2$ we have, for the time being, assumed that the shape of the efficiency curve for the furthest distance from the detector surface (4th position) is the same for all distances. The offsets for the closer positions, have been calculated from the measured efficiencies of ^{57}Co (^{57}Co showed very weak summation effects, see table 5). The corrected efficiencies, are also shown in fig. 7 (full lines). These corrected values of the efficiencies have been used for the calculation of the neutron yields in eq. [12].

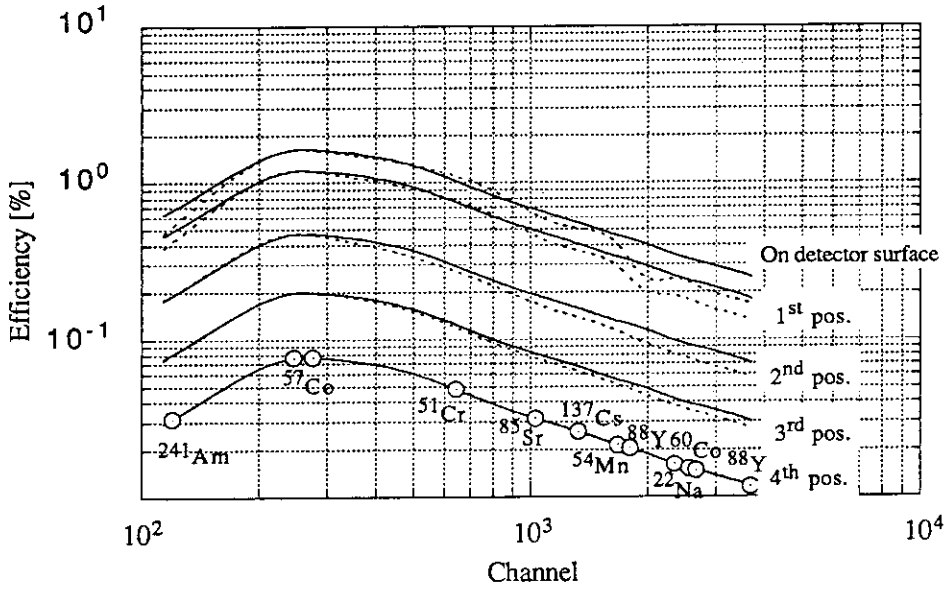

Fig.7. Efficiency of the HP-Ge detector as a function of channel (~0.5 keV/Channel). The non corrected (dotted lines) and corrected (full lines) efficiencies are shown for different source-detector distances. The curves are cubic-spline interpolated. It is evident that summation effects decreases with source-detector distance. The error of the efficiency for the 1st position is assumed to be ~10%. This error is reduced for positions further away from the detector.

4. Results

During the high β_p-phase at JT-60U, 27-30 July -93, approximately 100 samples were irradiated. We could not obtain any useful γ-counts from the nickel foil or from the reaction $^{27}Al(n,\alpha)^{24}Na$ (*cf.* table 1). The rest of the reactions, listed in table 1, gave useful γ-counts. The detection of the 2.5 MeV neutrons, from fusion of deuterium, have been made using indium- and zinc- foils while the 14 MeV neutrons, from fusion between deuterium and tritium, have been measured by aluminium-($^{27}Al(n,p)^{27}Mg$), copper- and silicon foils.

The indium foils gave good results and seem to be ideal for the measurement of 2.5 MeV neutrons. The cross section is large, giving good statistics for the measurement of the 336 keV γ-line.

The $^{64}Zn(n,p)^{64}Cu$ reaction was very weak due to the low neutron cross section at 2.5 MeV, *cf.* figs. 2 and 4. Furthermore, the ^{64}Cu-nucleus decays by β^+, giving rise to 511 keV annihilation photons. As long as all β^+ annihilates in the sample, the γ-measurement should be reliable. However, in the case of thin samples, a substantial amount of β^+ may escape the foil, leading to annihilation in the surrounding material, giving too many measured γ-counts. Also important, is the value of the endpoint-energy of the β^+ energy spectrum. High endpoint-energies (or average energies) implies that a large amount of β^+ may escape the sample. As a "rule of thumb", 1500 keV is considered to be a maximum critical value of the endpoint energy. The endpoint energy of β^+ from ^{64}Cu is ~650 keV which is far below the critical energy but, unfortunately, are the foils very thin (quadratic shaped: ~1 cm side length and < 0.2 mm thickness).

There are also 511 keV annihilation photons from the background. This background has been measured twice, under a period of 2-3 days. The background was 0.007+/-0.001 cps and has been subtracted in the measurements.

Further complicating factors are the following competing reactions:

$^{64}Zn(n,\gamma)^{65}Zn$, $t_{1/2}$ = 244.1 days (511 keV)

and

$^{64}Zn(n,2n)^{63}Zn$ $t_{1/2}$ = 38.1 min. (511 keV)

These reactions also contribute to the measured 511 keV photons. The contribution from the short-lived ^{63}Zn can be avoided by starting the γ-measurement ~5 hr's after the irradiation. However, the contribution from the long-lived ^{65}Zn must be corrected for. This can be achieved by making two measurements. The first measurement register the decays from both ^{64}Cu and ^{65}Zn. The second measurement should be done when the short-lived (12.7 hours) contribution from ^{64}Cu can be assumed to be negligible, *i.e.* only the contribution from ^{65}Zn is measured. The measured "true" counts can be calculated as follows:

In the first measurement from t_1 to t_2 (Δt_{21}), the measured 511 keV γ-counts from ^{64}Cu (C_{11}) and ^{65}Zn (C_{12}) can be written as (*cf.* eq. [4]):

$$C_1 = \underbrace{\alpha_{\gamma_1}\varepsilon\int_{t_1}^{t_2} A_{01}e^{-\lambda_1 t}dt}_{C_{11}} + \underbrace{\alpha_{\gamma_2}\varepsilon\int_{t_1}^{t_2} A_{02}e^{-\lambda_2 t}dt}_{C_{12}} + B\cdot\Delta t_{21} \qquad [20]$$

where B is the background count rate (0.007 cps).

In the second measurement from t_3 to t_4 (Δt_{43}), the contribution from ^{64}Cu (C_{21}) and ^{65}Zn (C_{22}) is:

$$\begin{aligned} C_2 &= \underbrace{\alpha_{\gamma_1}\varepsilon\int_{t_3}^{t_4} A_{01}e^{-\lambda_1 t}dt}_{C_{21}\approx 0} + \underbrace{\alpha_{\gamma_2}\varepsilon\int_{t_3}^{t_4} A_{02}e^{-\lambda_2 t}dt}_{C_{22}} + B\cdot\Delta t_{43} \\ &\approx \underbrace{\alpha_{\gamma_2}\varepsilon\int_{t_3}^{t_4} A_{02}e^{-\lambda_2 t}dt}_{C_{22}} + B\cdot\Delta t_{43} \end{aligned} \qquad [21]$$

$C_{21} \approx 0$ if $t_3 - t_1 \geq 10\cdot\dfrac{\ln 2}{\lambda_1}$ (~5 days for the zinc foil).

From eq. [21] we get:

$$\frac{\alpha_{\gamma_2}\varepsilon A_{02}}{\lambda_2} = \frac{C_2 - B\cdot\Delta t_{43}}{e^{-\lambda_2 t_3}\cdot(1-e^{-\lambda_2\Delta t_{43}})} \qquad [22]$$

From eq. [20] we get:

$$\begin{aligned} C_{11} &= (C_1 - B\cdot\Delta t_{21}) - C_{12} \\ &= (C_1 - B\cdot\Delta t_{21}) - \underbrace{\frac{\alpha_{\gamma_2}\varepsilon A_{02}}{\lambda_2}}_{Eq.[22]} e^{-\lambda_2 t_1}\cdot(1-e^{-\lambda_2\Delta t_{21}}) \\ &= (C_1 - B\cdot\Delta t_{21}) - (C_2 - B\cdot\Delta t_{43})\cdot e^{\lambda_2\Delta t_{31}}\cdot\frac{1-e^{-\lambda_2\Delta t_{21}}}{1-e^{-\lambda_2\Delta t_{43}}} \end{aligned} \qquad [23]$$

where Δt_{31} is the time between the starts of the two measurements, $\Delta t_{31} = t_3 - t_1$.

The corrected number of counts, C_{11}, is then used in eq. [12] for the calculation of the total 2.5 MeV neutron yield.

The reason for using zinc, in the first place, is the potential to obtain a measurement of an average neutron energy. If an indium and a zinc foil are irradiated simultaneously, then an average neutron energy may, in principle, be determined by the measurement of the fraction of γ-counts between indium and zinc. This fraction should be proportional to the difference in cross sections, *cf.* fig. 2. This measurement has not yet been done.

Figure 8 shows the measured 2.5 MeV neutron yield compared to the total neutron yield obtained from fission chambers. Generally, the obtained neutron yield from activation of indium is 10-20% higher. The neutron yields from zinc are even higher, probably due to the sensitivity of 14 MeV neutrons (*cf.* table 2). The error of the neutron yield measured by the fission chamber is ~10%. The error bars of the neutron yield from the indium foils are ~10-15% while the errors of the zinc measurements are ~20-25%.

50% of the fusion between deuterium atoms (D) gives tritons (T):

$$D + D \rightarrow T(1.011\ MeV) + p(3.022\ MeV)$$

For typical operating conditions at JT-60U, a small amount of the tritons will be confined, slowed down and thermalized. Whilst slowing down, there is a probability of about 1% that the triton may undergo a D-T fusion reaction ("triton burnup") thereby generating a 14 MeV neutron. The 14 MeV neutrons have been measured by activating ^{28}Si, ^{27}Al and ^{63}Cu. The activation of silicon and aluminium foils gave reasonable γ-counting statistics. The irradiation of copper give 511 keV photons and furthermore has the following competing reactions which must be corrected for:

$^{63}Cu(n,\gamma)^{64}Cu$ $\quad t_{1/2}$ = 12.7 hr's $\quad$ (511 keV)

and

$^{65}Cu(n,2n)^{64}Cu$ $\quad t_{1/2}$ = 12.7 hr's $\quad$ (511 keV)

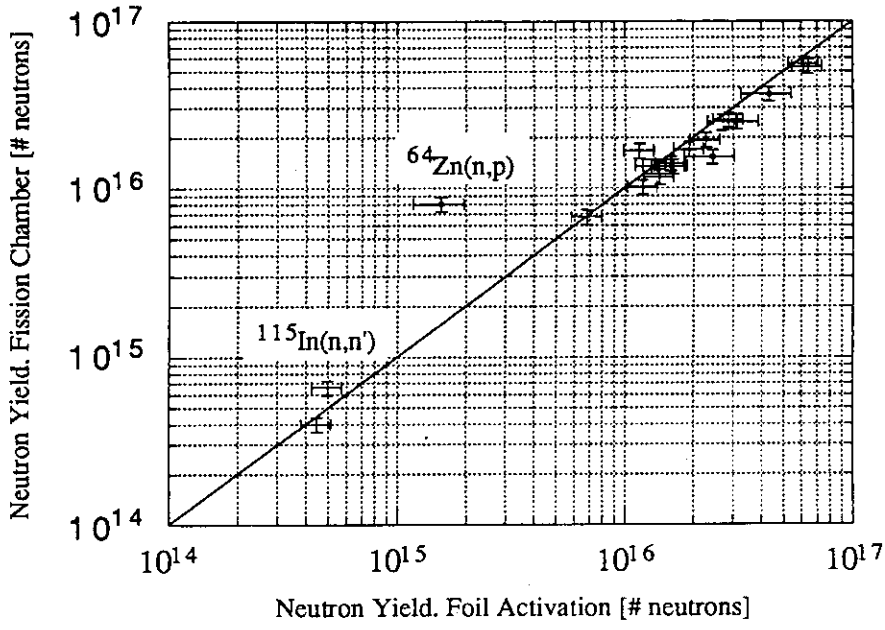

Fig.8. *Comparison between time-integrated neutron-yield from fission chamber and foil activation of indium and zinc. The obtained neutron yields from foil activation are generally 10-20% higher than those obtained from the fission chamber. The errors from the four zinc measurements are ~20-25% while the errors from the indium measurements are ~10-15%. The reason for the large deviation of one of the zinc measurements is unknown.*

As mentioned before, the endpoint energy of the β^+ decay from ^{64}Cu is ~650 keV. This means that β^+ annihilation in surrounding materials should be negligible, especially as the copper samples are thick (circular shaped with 1 cm diameter and 0.5-1.0 mm thickness). However, the endpoint energy of the β^+ radiation from the interesting reaction, ^{63}Cu(n,2n)^{62}Cu, is considerably higher, ~2.9 MeV, introducing large errors of the number of γ-counts.

The procedure for the correction, are similar to the zinc measurements where two measurements are done. In the first measurement, from t_1 to t_2, the measured 511 keV γ-counts from ^{62}Cu (C_{11}), ^{64}Cu$_1$ (C_{12}) and ^{64}Cu$_2$ (C_{13}) can be written as:

$$C_1 = \underbrace{\alpha_{\gamma_1}\varepsilon\int_{t_1}^{t_2} A_{01}e^{-\lambda_1 t}dt}_{C_{11}} + \underbrace{(\alpha_{\gamma_2}A_{02} + \alpha_{\gamma_3}A_{03})\varepsilon\int_{t_1}^{t_2} e^{-\lambda_2 t}dt}_{C_{12}+C_{13}} + B\cdot\Delta t_{21} \qquad [24]$$

In the second measurement from t_3 to t_4, the contribution from ^{62}Cu (C_{21}), $^{64}Cu_1$ (C_{22}) and $^{64}Cu_2$ (C_{23}) is:

$$C_2 = \underbrace{\alpha_{\gamma_1}\varepsilon\int_{t_3}^{t_4} A_{01}e^{-\lambda_1 t}dt}_{C_{21}\approx 0} + \underbrace{(\alpha_{\gamma_2}A_{02} + \alpha_{\gamma_3}A_{03})\varepsilon\int_{t_3}^{t_4} e^{-\lambda_2 t}dt}_{C_{22}+C_{23}} + B\cdot\Delta t_{43}$$

$$\approx \underbrace{(\alpha_{\gamma_2}A_{02} + \alpha_{\gamma_3}A_{03})\varepsilon\int_{t_3}^{t_4} e^{-\lambda_2 t}dt}_{C_{22}+C_{23}} + B\cdot\Delta t_{43} \qquad [25]$$

$C_{21} \approx 0$ if $t_3 - t_1 \geq 10\cdot\dfrac{\ln 2}{\lambda_1}$ (~2 hours for the copper foil).

It can then be shown that we get the same expression for the number of corrected γ-counts as eq. [23].

The measurement of the 14 MeV neutron yield utilizing aluminium and silicon foils are straightforward with only one measurement.

Figure 9 shows the results of the ratio [%] between 14 and 2.5 MeV neutrons ("T/D-fraction") plotted versus the plasma current. The error bars of the copper-, aluminium- and silicon-foils are ~20-60%, ~15-20% and ~10-15%, respectively (see section "Error Analysis"). The errors of the plasma current comes from the fact that during the time of the neutron burst, the plasma current is ramped up. The measurement of the neutron yield is time integrated and therefore an average value of the plasma current has been given in the figure.

It is not possible to draw any conclusions from fig. 9 due to the few data. However, one can expect that the confinement of the tritons should increase with increased plasma current and this tendency (with a few exceptions) can be seen in the figure.

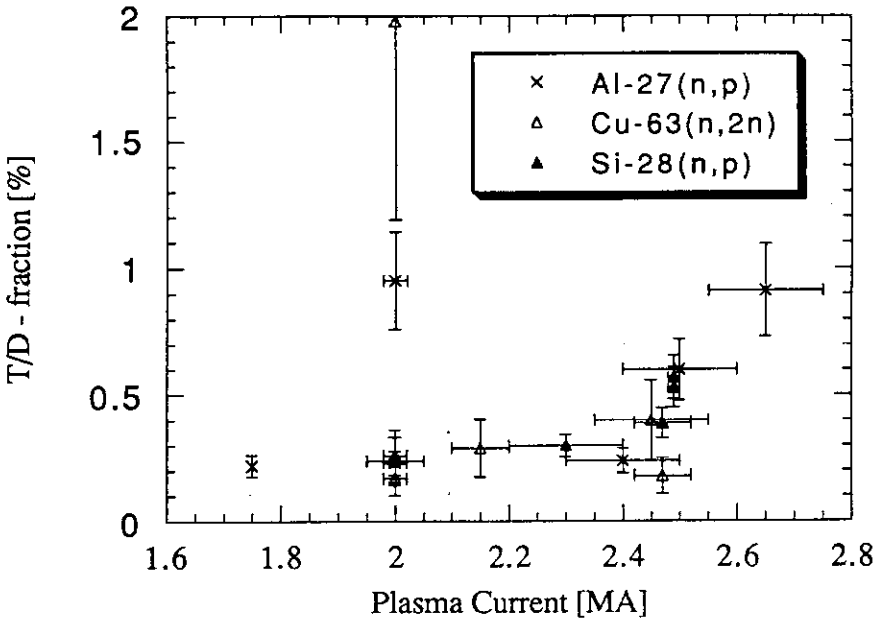

Fig.9. Ratio between 14 and 2.5 MeV neutrons. The fractions are generally centered around 0.5% and tends to increase with increased plasma current, indicating a better confinement of the tritons.

5. Error Analysis

The dominant errors for the calculation of the neutron yield, *cf.* eq. [12], are the values of the measured γ-counts, C, the efficiency of the γ-detector, ε, and the value of the flux integral, F. Using the error propagation formula, we get the following expression for the error of the neutron yield, σ_{S_n}:

$$\begin{aligned}\sigma_{S_n}^2 &= \left(\frac{\partial S_n}{\partial C}\right)^2 \sigma_C^2 + \left(\frac{\partial S_n}{\partial \varepsilon}\right)^2 \sigma_\varepsilon^2 + \left(\frac{\partial S_n}{\partial F}\right)^2 \sigma_F^2 \\ &= S_n^2 \left[\left(\frac{\sigma_C}{C}\right)^2 + \left(\frac{\sigma_\varepsilon}{\varepsilon}\right)^2 + \left(\frac{\sigma_F}{F}\right)^2 \right]\end{aligned} \qquad [26]$$

where

$$F = \sum_i \Phi^*(E_i) \cdot \sigma(E_i) \equiv \sum_i \Phi_i^* \cdot \sigma_i . \qquad [27]$$

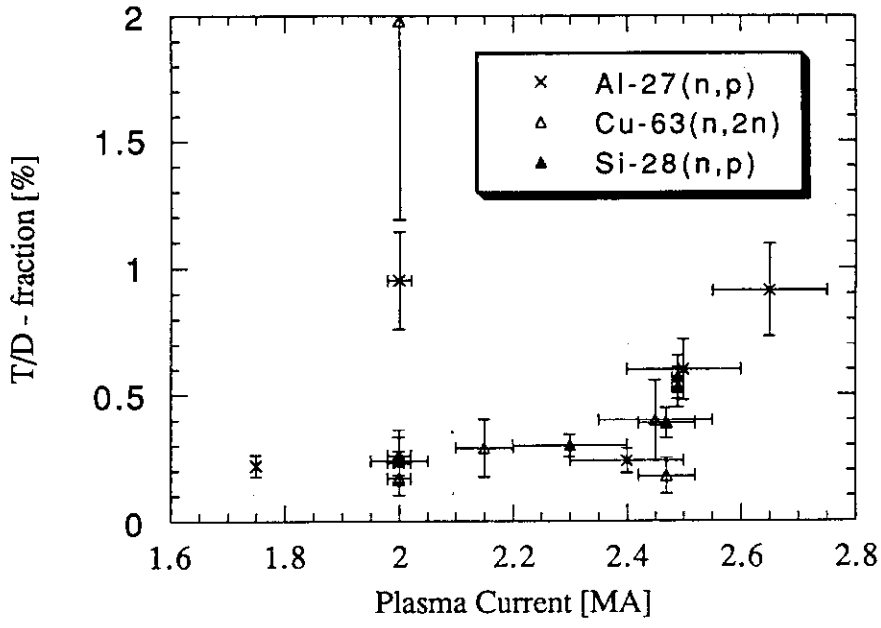

Fig.9. Ratio between 14 and 2.5 MeV neutrons. The fractions are generally centered around 0.5% and tends to increase with increased plasma current, indicating a better confinement of the tritons.

5. Error Analysis

The dominant errors for the calculation of the neutron yield, *cf.* eq. [12], are the values of the measured γ-counts, C, the efficiency of the γ-detector, ε, and the value of the flux integral, F. Using the error propagation formula, we get the following expression for the error of the neutron yield, σ_{S_n}:

$$\begin{aligned}\sigma_{S_n}^2 &= (\frac{\partial S_n}{\partial C})^2 \sigma_C^2 + (\frac{\partial S_n}{\partial \varepsilon})^2 \sigma_\varepsilon^2 + (\frac{\partial S_n}{\partial F})^2 \sigma_F^2 \\ &= S_n^2 \left[(\frac{\sigma_C}{C})^2 + (\frac{\sigma_\varepsilon}{\varepsilon})^2 + (\frac{\sigma_F}{F})^2 \right]\end{aligned} \qquad [26]$$

where

$$F = \sum_i \Phi^*(E_i) \cdot \sigma(E_i) \equiv \sum_i \Phi_i^* \cdot \sigma_i . \qquad [27]$$

The error of the number of γ-counts, σ_C, varies between the samples, depending on the "neutron sensitivity" of the foil (*cf.* figs. 4 and 5), but also within the same type of samples, depending on the total emitted neutron yield. Table 6 shows some measurements, where the number of γ-counts and their corresponding error is indicated. The indicated counts are corrected for background under the peak (*e.g.* the Compton distribution background). However, the 511 keV background (0.007 +/- 0.001 cps), important for the zinc and copper foils, are not indicated. Instead of a calculated error for each measurement, we have, for the time being, chosen to assume a constant percentile error, ε_C, of the counts, common for all measurements. This error is shown in the last column of table 6.

Table 6. *Net area (corrected for background) with the error for a few measurements. Columns 4 and 5, shows the net area and error for those foils where two measurements are necessary. In-115 (1-3) is the same indium foil, measured three times but at different cooling times; (1), immediately after irradiation and (3), after a cooling time of ~5hr's. The last column shows the assumed error of the γ-counts, common for all measurements. The large assumed errors for copper and zinc, are motivated by the difficulty of the measurement of the 511 keV photons.*

Foil	Net Area [Counts]	Error [%]	Net Area (2) [Counts]	Error [%]	Assumed Error
In-115	142	14.1			
In-115	4569	1.9			
In-115 (1)	989	23.1			
In-115 (2)	8392	4.2			
In-115 (3)	5745	1.9			< 5%
Zn-64	155	9.7	81	23.5	
Zn-64	779	5.3	552	11.2	
Zn-64	1717	2.7	1411	8.3	
Zn-64	5468	1.8	938	9.2	< 20%
Al-27 (n,p)	106	22.6			
Al-27 (n,p)	291	12.7			
Al-27 (n,p)	731	7.4			< 15%
Cu-63	3960	2.1	3462	1.8	
Cu-63	5542	1.8	169949	0.3	
Cu-63	9832	1.6	43685	0.5	
Cu-63	10483	1.2	8944	1.2	< 10%
Si-28	118	9.3			
Si-28	150	9.3			
Si-28	170	8.2			
Si-28	228	7.0			< 10%

When two measurements of the γ-counts are necessary (511 keV from zinc and copper foils), then the error of the number of γ-counts (including the error of the background, σ_B) σ_C in eq. [26], are modified according to (see eq. [23]):

$$\sigma_C^2 \equiv \sigma_{C_{11}}^2 = (\frac{\partial C_{11}}{\partial C_1})^2 \sigma_{C_1}^2 + (\frac{\partial C_{11}}{\partial C_2})^2 \sigma_{C_2}^2 + (\frac{\partial C_{11}}{\partial B})^2 \sigma_B^2$$

$$= \sigma_{C_1}^2 + (-e^{\lambda_2 \Delta t_{31}} \cdot \frac{1-e^{-\lambda_2 \Delta t_{21}}}{1-e^{-\lambda_2 \Delta t_{43}}})^2 \sigma_{C_2}^2 + \qquad [28]$$

$$+(-\Delta t_{21} + \Delta t_{43} \cdot e^{\lambda_2 \Delta t_{31}} \cdot \frac{1-e^{-\lambda_2 \Delta t_{21}}}{1-e^{-\lambda_2 \Delta t_{43}}})^2 \sigma_B^2$$

where

$$\sigma_{C_1} \approx \varepsilon_{C_1} \cdot C_1$$
$$\sigma_{C_2} \approx \varepsilon_{C_2} \cdot C_2 \qquad [29a\text{-}c]$$
$$\varepsilon_{C_1} \approx \varepsilon_{C_2} \equiv \varepsilon_C$$

and where ε_C is obtained from table 6. B is the 511 keV background count rate.

For the measurements done so far, the errors of the number of γ-counts have been 15-60% (not shown in table 6) and ~20% for copper and zinc, respectively.

The error of the efficiency of the γ-detector, σ_ε, is not known. The error due to the limited number of measured counts from the calibration sources can easily be calculated, but the error due to the unknown effect from summation effects is probably much larger. However, we have assumed that the error is better than 10% at the 1st measurement position. For measurement positions further away from the γ-detector, this error is considerably reduced due to the reduced effects from summation.

The error of the flux integral depends on the errors of both the cross sections and the calculated flux from MCNP. The errors of the flux, $\sigma_{\Phi_i^*}$, can be obtained from MCNP. However, these errors are statistical errors from the Monte Carlo calculations and are probably negligible compared to the "real" errors. If we assume a constant percentage value, ε, of the error of both the flux, $\sigma_{\Phi_i^*} \approx \varepsilon_{\Phi^*} \cdot \Phi_i^*$, and the cross section, $\sigma_{\sigma_i} \approx \varepsilon_\sigma \cdot \sigma_i$, then we can express the error of the flux integral as:

$$\sigma_F^2 = \sum_i \left[\underbrace{\left(\frac{\partial F}{\partial \Phi_i^*}\right)^2}_{\sigma_i} \sigma_{\Phi_i^*}^2 + \underbrace{\left(\frac{\partial F}{\partial \sigma_i}\right)^2}_{\Phi_i^*} \sigma_{\sigma_i}^2 \right]$$

$$= \sum_i \left[(\sigma_i \sigma_{\Phi_i^*})^2 + (\Phi_i^* \sigma_{\sigma_i})^2 \right] \qquad [30]$$

$$= (\varepsilon_{\Phi^*}^2 + \varepsilon_\sigma^2) \cdot \sum_i (\sigma_i \Phi_i^*)^2$$

$\sigma_{\Phi_i^*}$ have been estimated to ~10%, which is the same value as the error of the obtained neutron yield from the fission chambers. The errors of the cross sections, σ_σ, which have been obtained from FNS [5], are ~5% per energy group. When the errors are calculated according to eq. [30], generally, the errors of the flux integrals are less than 10%.

The conclusions from the error analysis and the measurements done so far, are that for the measurement of the 2.5 MeV neutron yield, indium should give the best overall error (10-15%). Using zinc gives a larger error mainly because of the uncertainty in the measurement of the number of γ-counts. The overall error of the neutron yield obtained using zinc is ~20-25%.

For the measurement of the 14 MeV neutron yield, the silicon sample should give the lowest error (10-15%) of the neutron yield while the aluminium sample gives ~15-20% error. Using copper may give very large errors and should be done with caution.

6. Summary

The neutron yield measurements at JT-60U have now been complemented by foil-activation technique. A sample is exposed to a flux of neutrons for a period of time, and then removed by a rabbit system, to a γ-detector where the induced radioactivity is measured.

The main advantage of foil activation is that the samples can be positioned very close to the plasma without any regards of radiation damages to detectors or electronics. Furthermore, the necessary equipment is simple and reliable. The main disadvantage is that every measurement have to be done manually and an automatic procedure is not trivial.

The neutron activation system has recently been installed and good agreement of the measurements of the 2.5 MeV neutron yield from foil activation and fission chambers has been shown. Furthermore, the fractions between 14 MeV and 2.5 MeV neutrons have been measured for a few pulses and seem to yield reasonable values.

The dominant errors for the calculation of the neutron yield, are the values of the measured γ-counts, the efficiency of the γ-detector and the value of the flux integral. If it is assumed that the errors of the efficiency of the detector and the Monte Carlo calculated neutron flux are ~10%, then the errors of the measured 2.5 MeV neutron yield, utilizing indium and zinc, are ~10-15% and ~20-25%, respectively. For the measurement of the 14 MeV neutron yield, the estimated errors for silicon, aluminium ($^{27}Al(n,p)^{27}Mg$) and copper are ~10-15%, ~15-20% and ~20-60% respectively. The large errors utilizing zinc and copper foils, are mainly due to the difficulty in the measurement of the annihilation radiation.

The experience has shown that for the measurements of the 2.5 MeV neutron yields, $^{115}In(n,n')^{115m}In$ is the most suitable reaction. For the measurement of 14 MeV neutrons, utilizing $^{28}Si(n,p)^{28}Al$ and $^{27}Al(n,p)^{27}Mg$, give best results (relatively small errors).

Future work includes a number of actions:

- Optimization of cooling times of the activated foils,
- Improvement of the efficiency calculations for the HP-Ge detector. In almost all cases, the activated foil is measured at the first position (*cf.* fig. 7). An improved efficiency calculation will probably deviate to a large extent from the present "guessed" efficiency curve,
- Estimation of neutron "screening" effects by the measurement of several identical foils and Monte Carlo calculations (MCNP),
- Estimation of an average neutron energy using indium and zinc foils simultaneously,
- Compare measured T/D-fractions with results from SBD detector,
- Measurements of more than one "14 MeV foil" simultaneously to obtain the T/D-fraction uncertainty between different foils,
- Estimation of triton losses using results from foil activation and Monte Carlo simulation of triton losses using the OFMC code.

Acknowledgment

One of us (MH), would like to express his gratitude to Science and Technology Agency (STA) for the granted STA postdoctoral fellowship.

References

[1] T. Nishitani, H. Takeuchi, C.W. Barnes and T. Iguchi.
Japan Atomic Energy Research Institute Report JAERI-M 92-073 (1993), pp. 234-237.

[2] Los Alamos Monte Carlo Group, LANL Report LA-7396-M, Rev.2 (1986)

[3] T. Nishitani, A. Morioka and Y. Ikeda.
Japan Atomic Energy Research Institute Report JAERI-M 93-057 (1993), pp. 267-270.

[4] T. Nishitani and Y. Ikeda.
Japan Atomic Energy Research Institute Report JAERI-M 92-073 (1992), pp. 242-245.

[5] Y. Ikeda et al.
Japan Atomic Energy Research Institute Report JAERI 1312 (1988)

[6] Laboratoire de Mesures des Rayonnements Ionisants, DAMRI/LMRI BP 52-91193 Gif-Sur-Yvette Cedex France

Acknowledgment

One of us (MH), would like to express his gratitude to Science and Technology Agency (STA) for the granted STA postdoctoral fellowship.

References

[1] T. Nishitani, H. Takeuchi, C.W. Barnes and T. Iguchi.
Japan Atomic Energy Research Institute Report JAERI-M 92-073 (1993), pp. 234-237.

[2] Los Alamos Monte Carlo Group, LANL Report LA-7396-M, Rev.2 (1986)

[3] T. Nishitani, A. Morioka and Y. Ikeda.
Japan Atomic Energy Research Institute Report JAERI-M 93-057 (1993), pp. 267-270.

[4] T. Nishitani and Y. Ikeda.
Japan Atomic Energy Research Institute Report JAERI-M 92-073 (1992), pp. 242-245.

[5] Y. Ikeda et al.
Japan Atomic Energy Research Institute Report JAERI 1312 (1988)

[6] Laboratoire de Mesures des Rayonnements Ionisants, DAMRI/LMRI BP 52-91193 Gif-Sur-Yvette Cedex France